Journal of Power Sources 233 (2013) 380–393

Contents lists available at SciVerse ScienceDirect

Journal of Power Sources

journal homepage: www.elsevier.com/locate/jpowsour

# Techno-economic analysis of solid oxide fuel cell-based combined heat and power systems for biogas utilization at wastewater treatment facilities

A.A. Trendewicz, R.J. Braun*

*Department of Mechanical Engineering, College of Engineering and Computational Sciences, Colorado School of Mines, 1610 Illinois Street, Golden, CO 80401, USA*

## HIGHLIGHTS

- ► SOFC systems fueled with biogas offer net electrical efficiencies near 52% (LHV).
- ► Estimated installed costs range from 3590 $/kW to 5780 $/kW (large- to small-scale).
- ► SOFC-based cost of electricity is competitive with grid-pricing at 5–8 ¢/kW h.
- ► SOFCs for biogas applications are competitive with other cogeneration technologies.
- ► Economic viability also depends on biogas quality, utility pricing, and incentives.

## ARTICLE INFO

*Article history:*
Received 23 August 2012
Received in revised form
29 November 2012
Accepted 3 January 2013
Available online 13 January 2013

*Keywords:*
SOFC
CHP
Biogas
Wastewater treatment
Techno-economics

## ABSTRACT

This paper presents a techno-economic analysis of biogas-fueled solid oxide fuel cell (SOFC) systems for combined heat and power (CHP) applications in wastewater treatment facilities (WWTFs). SOFC-CHP systems ranging from 300 kWe to 6 MWe in electric power capacity are explored in terms of their performance and life cycle costs. Representative biogas feedstock is established from compositional data for a large wastewater reclamation facility in Denver, Colorado. A steady-state SOFC-CHP system model is developed with Aspen Plus for the integration with small (640 $kW_{LHV}$), medium (2.97 $MW_{LHV}$) and large (11.92 $MW_{LHV}$) biogas sources. The proposed SOFC system concept includes anode gas recirculation, a biogas pretreatment system, and a waste heat recovery unit. The system offers a net electrical efficiency of 51.6% LHV and a net CHP efficiency of 87.5% LHV. The effect of operating parameters on system efficiency is investigated with a parametric study. The economic performance is evaluated with the levelized costs of electricity (COE) and heat (COH). The results are compared with the COE from reciprocating engine, gas turbine, microturbine, molten carbonate fuel cell technologies, and grid electricity prices. The influence of economic parameters and stack operating parameters on the levelized COE is also presented.



## 1. Introduction

Biogas is a mixture of methane and carbon dioxide with trace amounts of other compounds. It is produced by anaerobic digestion (AD) of waste streams containing organic matter, such as wastewater, animal waste, food waste, or landfills. Biogas composition varies depending on the properties of the feedstock. The biogas from wastewater, animal waste, or food waste typically consists of 50–70% $CH_4$, 30–50% $CO_2$, and 0–6% $H_2O$ [1]. The commonly encountered contaminants are hydrogen sulfide, $H_2S$ (0–10,000 ppmv) [1] and silicon compounds (200–10,000 ppbv) [2]. Landfill gas is comprised of 40–55% $CH_4$, 35–50% $CO_2$, 0–20% $N_2$ [1], 0–6% $H_2O$ and it is usually highly contaminated with $H_2S$, silicon compounds, halogens and heavy metals [3].

The interest in biogas utilization as a fuel stems largely from its high methane content, renewable status, relatively low feedstock cost, and increasing resource potential (due to population growth). One way to assess biogas resource potential is to examine the methane emissions from various waste sources. The total methane emissions in the United States in 2009 were estimated to equal about 730.9 million metric tons of $CO_2$ equivalent ($MTCO_{2e}$) [4]. The distribution of methane emissions among various sources is summarized in Table 1. About 41.5% of the total methane emissions in the U.S. come from fossil energy sources (natural gas production,

* Corresponding author. Tel.: +1 303 273 3055; fax: +1 303 273 3602.
*E-mail addresses:* atrendew@mines.edu (A.A. Trendewicz), rbraun@mines.edu (R.J. Braun).

0378-7753/$ – see front matter © 2013 Elsevier B.V. All rights reserved.
http://dx.doi.org/10.1016/j.jpowsour.2013.01.017

processing, storage and distribution, coal mining, petroleum refining, combustion systems), 29.5% from agriculture (animal waste, rice cultivation and crop residue burning), 28.4% from waste management (landfills, domestic wastewater treatment, and industrial wastewater treatment) and 0.6% from industrial processes (chemical production, iron and steel production).

While animal waste and landfills have the highest biogas potential, the focus of this study is on biogas generated at WWTFs, as they are an attractive niche market for fuel cells. In particular, they offer the possibility of operating an SOFC system in a combined heat and power (CHP) mode, since there is a significant onsite heat load due to the anaerobic digesters. There are over 16,000 municipal WWTFs in the United States and around 1000 of those facilities have a wastewater flow larger than 114 $m^3\ s^{-1}$ [5]. Only 60% of the wastewater flow from the aforementioned facilities (>114 $m^3\ s^{-1}$) is conveyed to wastewater facilities equipped with anaerobic digesters (AD). Furthermore, only 20% of the facilities with ADs actually utilize the produced biogas [5]. An overview of the biogas potential at WWTFs is presented in Table 2.

Small WWTFs are the most numerous group with the highest total wastewater flow (189,717 $m^3\ s^{-1}$). Only 45% of the wastewater flow directed to small plants is processed in anaerobic digesters to produce biogas. This is because integrating an AD is capital intensive, and it is often not economically favorable at a small scale [2]. Digesters become more common with an increase in the size of a wastewater processing plant. In addition to the economy of scale, the digestion process becomes more efficient, and the average amount of biogas ($MW_{LHV}$) generated from 22.82 $m^3\ s^{-1}$ of wastewater increases from 80 $kW_{LHV}$ at small facilities to 95 $kW_{LHV}$ at medium facilities, and 110 $kW_{LHV}$ at large and very large plants [6]. The total estimated theoretical biogas potential (assuming all the wastewater is processed in ADs) is 2581 MW.

There are currently 104 WWTFs which employ CHP systems fueled with biogas [5]. The total installed capacity of those systems is 190 MWe. The most popular technology is reciprocating engines representing approximately 45% of the installed capacity (see Table 3). Gas turbines and steam turbines are a common choice for large scale applications accounting for approximately 48% of the total installed capacity. There is still a significant unexploited biogas potential associated with WWTFs which could be leveraged to substitute fossil fuels currently used for power generation, heat generation, or transportation. The possible biogas utilization pathways are summarized in Fig. 1.

After pretreatment, defined as contaminants removal, biogas can be sold as a fuel to an industrial user (where possible). This is the least capital intensive investment option for biogas utilization. Another pathway is to upgrade the biogas to a pipeline quality natural gas by removing contaminants and excessive $CO_2$, compress it, and sell it to a local utility or use it onsite as a vehicle fuel (CNG). This utilization pathway requires an advanced biogas upgrading system. The economic viability of bio-methane production depends on the natural gas price, renewable fuel standards (RFS) and related renewable fuel incentives, such as renewable identification number (RIN) [7]. Other potentially attractive applications for biogas include heat generation in a boiler, combined heat and power generation in a reciprocating engine, a gas turbine or a fuel cell system, and combined heat, hydrogen and power (CHHP) generation in a fuel cell system [40]. The CHP distributed generation pathway is particularly attractive due to its high overall conversion efficiency and onsite integration options. Onsite cogeneration offers a reduction in both the use of fossil fuels for heat generation and the grid electricity demand. Among the available distributed cogeneration technologies, fuel cells offer the highest electrical efficiency and the lowest pollutant emissions [2].

Interest in fuel cell systems for biogas utilization at WWTFs began in the 1990s when the first commercial phosphoric acid fuel cell (PAFC) systems were implemented [8]. At present, MCFCs and SOFCs are receiving increased attention due to their higher electrical efficiency and higher tolerance to contaminants compared with PAFCs. Biogas-fueled MCFCs are close to commercialization with several megawatts of installed capacity at WWTFs in California [1]. SOFC technology is also being commercialized with several companies launching product lines, yet only one OEM offers a product at the scale congruent with WWTF applications. Research and development on SOFCs for biogas has focused mostly on single cell performance (with an emphasis on establishing allowable operating conditions [9]), biogas reforming methods [10], the effect of contaminants on the nickel catalyst activity [11–13], and small-scale system tests [14]. The performance of large-scale biogas-fueled SOFC systems is evaluated mostly with computer modeling [15,16]. Industrial efforts toward commercialization of SOFC technology for biogas applications have ranged from operation of a 20 kW pilot plant on landfill gas [3] to a 6 MW plant planned for a data center [17]. Although the technical performance of SOFC units on biogas fuel is promising, little is known about the economic potential of such systems.

The objective of this paper is to investigate the technical and economic benefits of the cogeneration pathway for biogas utilization with focus on solid oxide fuel cell (SOFC) technology. The technical performance of a hypothetical SOFC system employing anode gas recycling (AGR) is evaluated with an Aspen Plus

**Table 1**
Methane emissions by source in the United States in 2009 [4].

| Source | $CH_4$ ($MTCO_{2e}$) | %Total |
|---|---|---|
| Energy sources | 303.0 | 41.5 |
| Animal waste | 203.2 | 27.8 |
| Landfills | 179.7 | 24.6 |
| Domestic wastewater | 17.8 | 2.4 |
| Rice and crops | 12.6 | 1.7 |
| Industrial wastewater | 10.4 | 1.4 |
| Industrial processes | 4.2 | 0.6 |

**Table 2**
An overview of the biogas potential at WWTFs in the US [5,6].

| WWTF size | Number of sites | Biogas potential per site (kW) | Total biogas potential (MW) | % Wastewater ($m^3\ s^{-1}$) to AD |
|---|---|---|---|---|
| Small (22.8–228 $m^3\ s^{-1}$) | 2713 | 80–800 | 665 | 45% |
| Medium (228–912 $m^3\ s^{-1}$) | 381 | 800–3800 | 716 | 59% |
| Large (912–2280 $m^3\ s^{-1}$) | 49 | 3800–11,000 | 401 | 70% |
| Very large (>2280 $m^3\ s^{-1}$) | 28 | >11,000 | 732 | 76% |
| Total | 3171 | – | 2581 | – |

**Table 3**
A summary of existing CHP facilities at WWTFs in the US [5].

| Technology | Number of sites | Capacity (MW) | Average capacity (kW) |
|---|---|---|---|
| Reciprocating engine | 54 | 85.8 | 1590 |
| Microturbine | 29 | 5.2 | 179 |
| Fuel cell | 13 | 7.9 | 609 |
| Gas turbine | 5 | 39.9 | 7980 |
| Steam turbine | 2 | 23 | 11,500 |
| Combined cycle | 1 | 28 | 28,000 |
| Total | 104 | 189.8 | 1825 |

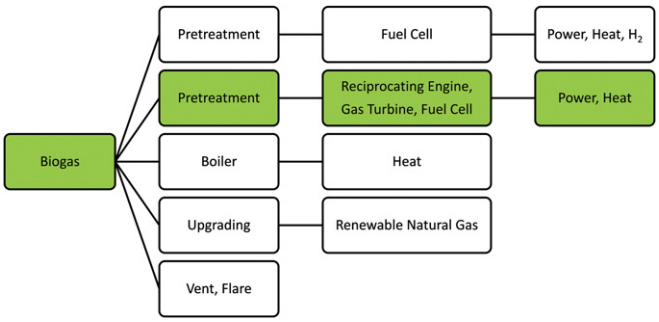


**Fig. 1.** Biogas utilization pathways.

computer model for the case of integration with small-, medium-, and large-scale-WWTFs. The input data for the model concerning biogas composition are acquired from the Metro Wastewater Reclamation Facility in Denver, Colorado. The effects of operating parameters, such as steam-to-carbon ratio ($S/C$), fuel utilization ($U_{F,sys}$), and the extent of external reforming (%ER) on system efficiency are presented. The economic performance of the proposed SOFC system is evaluated using life cycle costing methods expressed in terms of the levelized cost of electricity (COE). The results are subjected to a sensitivity analysis in order to evaluate the relative influence of the capital cost, the biogas cost, the capacity factor and operating parameters on system economics. The baseline COE from the SOFC system is compared with the COE for other technologies integrated within the same facility, such as MCFCs, reciprocating engines, and gas turbines. The comparative influence of the economy of scale on the economic viability for all technologies is established through the small, medium, and large-scale WWTF results.

## 2. Cogeneration technologies for biogas utilization

There are several prime mover technologies suitable for biogas utilization at WWTFs. The most commonly employed are reciprocating engines, gas turbines, microturbines, and fuel cells [2]. The choice of the technology for a particular application is dependent on the size of the biogas source, biogas contaminants levels, required fuel pretreatment, local utility pricing, local emissions regulations, and local incentives. It is generally estimated that cogeneration projects become economic at WWTFs with a minimum capacity of 228.24 $m^3\ s^{-1}$ [2]. However, the most recent estimates made by the EPA indicate that the cogeneration might be considered for facilities with wastewater flow of 114 $m^3\ s^{-1}$ [5]. The economics of cogeneration projects in small scale WWTFs can be improved by implementing a co-digestion of fats, oils, and grease (FOG) or food waste, which results in an increased biogas production [2]. The technical and economic indicators of biogas-fueled cogeneration plants are site specific due to the local character of biogas composition and flow rate. Therefore, when making a comparison between different cogeneration technologies, it is reasonable to present a range of performance characteristics as shown in Table 4.

Reciprocating engines and fuel cells offer high electrical efficiency and are well-suited for small-and medium-scale wastewater facilities. Gas turbines are generally better suited for large-scale WWTFs given the OEM product offerings on the market. Reciprocating engines are well-proven, optimized for biogas fuel (lean-burn engines) and commercially available from several manufacturers. Similarly to reciprocating engines, gas turbines are a well-proven and commercially available technology. However, gas turbines have a lower electrical efficiency, and they are highly sensitive to ambient conditions. Moreover, gas turbines require high inlet fuel pressure. Fuel compression can be costly and energy intensive. Microturbines are small-scale centrifugal gas turbines. They share many of the same characteristics of larger gas turbines, yet are often of lower efficiency. Fuel cells are highly efficient and offer relatively low pollution emissions compared with other technologies due to direct conversion of the chemical energy into electricity instead of combustion. Yet as an emerging technology, they are very capital-intensive. The total project cost of a biogas-fueled fuel cell system is further increased by the requirement of extremely high fuel purity which requires an extensive biogas pretreatment system.

## 3. Biogas pretreatment

In addition to $H_2S$ and siloxanes, biogas produced at WWTFs usually has high moisture content. The presence of water in biogas is generally desirable for both combustion devices and fuel cells. In combustion devices, water reduces the flame temperature and contributes to lower $NO_x$ emissions; in fuel cells, water is required for the steam reforming of methane (SMR). However, water is usually considered to be a contaminant in biogases. This is because it condenses in pipelines (when the temperature of saturated biogas drops) and reacts with hydrogen sulfide to form a highly corrosive sulfuric acid ($H_2SO_4$) [2]. In addition, the presence of liquid water in compressors is undesirable as it causes erosion of rotating blades [18]. Water is typically removed by cooling the saturated biogas in a heat exchanger, if necessary [2]. Hydrogen sulfide requires removal from the digester gas because of its corrosive nature. Moreover, in the combustion process, it forms oxides of sulfur ($SO_x$) which are air polluting [2]. If supplied to a high temperature fuel cell, $H_2S$ is highly poisonous to the nickel catalyst present in any pre-reformer or in the anode [11]. For successful SOFC applications the $H_2S$ concentration in biogas should be maintained below 2.82 mg $m^{-3}$ [3]. The most commonly employed hydrogen sulfide removal method is adsorption over a hydrated ferric oxide

**Table 4**
Comparison of cogeneration technologies for biogas utilization [2,18].

| Technology | Reciprocating engines | Gas turbines | Microturbines | Fuel cells |
|---|---|---|---|---|
| Size (kW) | 110–4400 | 600–22,000 | 30–250 | 100–2800 |
| $\eta_{electrical}$ (% LHV) | 30–42 | 19–34 | 26–30 | 36–50+ |
| $\eta_{heat\ recovery}$ (% LHV) | 35–49 | 40–52 | 30–37 | 30–40 |
| Fuel pressure (kPa) | 115–653 | 791–2859 | 618–791 | 239–308 |
| Equipment ($ $kW^{-1}$) | 465–1600 | 1100–2000 | 800–1600 | 3800–5280 |
| Cleanup ($ $kW^{-1}$) | 0–500 | 0–500 | 500–3000 | 500–3000 |
| O&M ($ kW $h^{-1}$) | 0.01–0.025 | 0.008–0.01 | 0.012–0.025 | 0.004–0.019 |
| Availability (%) | 90–96 | 95–97 | 85–90 | 90–95 |
| Overhaul (h) | 28,000–90,000 | 30,000–50,000 | 30,000–50,000 | 10,000–80,000 |
| NOx (g $GJ^{-1}$) | 6.45–374.1 | 43.43–120.4 | 51.6–81.7 | 1.29–2.58 |
| CO (g $GJ^{-1}$) | 70.09–928.8 | 52.89–212.4 | 223.6–756.8 | 2.58–6.88 |
| Example Manufacturers | Jenbacher, CAT, Waukesha | Solar, Kawasaki | Capstone, Ingersoll-Rand | UTC, Bloom Fuel Cell Energy |

or other catalytic media [2]. Industrial examples include SULFA-TREAT, Sulfur-Rite, and SULFA-BIND catalysts. Depending on the initial $H_2S$ concentration in biogas, a two-stage sulfur removal system might be required for a fuel cell system which greatly increases both the investment cost and the maintenance cost [19]. Siloxanes are highly volatile, large organic compounds comprised of silicon, oxygen and alkanes and are popular additives to cleaning agents. Thus their concentration in biogas produced at WWTFs is steadily increasing over time [20]. At high temperatures, siloxanes are oxidized to silica ($SiO_2$) which forms hard, glassy deposits on heat exchanger surfaces, engine valves or turbine blades [20]. This leads to an increased maintenance cost and more frequent overhauls. Silica is particularly dangerous to high temperature fuel cells as it might fill the porous structure of the anode and obstruct reactant gas transport. The most common siloxane removal method is adsorption over active carbon or silica gels. The adsorber is placed downstream of hydrogen sulfide and moisture removal processes as it tends to work more efficiently in the absence of competing species. The adsorption media are usually regenerated by temperature swing adsorption (TSA) or pressure swing adsorption (PSA). The siloxanes concentration in biogas for fuel cells application should be kept below 2.82 mg $m^{-3}$ [21].

## 4. Fluctuations in biogas production

The rate of biogas production at WWTFs is not constant and may vary both on seasonal and hourly time bases. Depending on the magnitude and rate of fluctuations in biogas production, the operation of reciprocating engines, gas turbines or fuel cells could be disrupted. The two most commonly implemented strategies for mitigating the effect of biogas production fluctuations are (1) to introduce a biogas storage system or (2) to supplement biogas deficiency with natural gas.

Biogas is typically stored only for short-terms (hourly) and at low pressures. This is because a long term storage system requires biogas pressurization. The energy input for biogas compression to a typical storage pressure of 1725 kPa (250 psi) is equal to approximately 10% of the energy value of stored biogas. Moreover, long term storage of biogas in pressurized cylinders requires contaminant removal (hydrogen sulfide, water) due to the danger of corrosion. The aforementioned requirements introduce an additional cost and make the long term storage of a low-calorific value biogas fuel unattractive. In contrast, short-term biogas storage options are low cost and easy to maintain. The two most commonly employed short-term biogas storage technologies are floating covers and gas bags. A floating cover is a double membrane storage tank mounted directly on an existing digester tank. A gas bag is an inflatable membrane placed in a separate rigid metal container in order to prevent it from being damaged. Both floating covers and gas bags are made of polyethylene, which is a low cost material.

Blending supplemental natural gas fuel with biogas has an influence on both the technical performance and the economics of an SOFC system. The addition of natural gas to biogas results in an increased concentration of methane in the feed stream to the onsite power plant. This causes an increased cell voltage and higher power output from an SOFC system at constant fuel utilization. However, there is a trade-off in the form of additional fuel cost. Therefore, estimating the influence of blending biogas with natural gas on the techno-economics of an SOFC system requires some information about the magnitude and duration of biogas production rate fluctuations.

It is difficult to predict fluctuations in biogas production as they depend on wastewater flow rates, the activity of bacteria and operating conditions of the digesters. Based on the data acquired from the Metro Wastewater Treatment facility in Denver, it is observed that fluctuations of the biogas energy production at the facility are generally within 20% of the average biogas energy production over short intervals (based on 1-week data sets using 15 min average values) and within 10% of the biogas energy production over longer intervals (based on monthly average values) [24], as shown in Figs. 2 and 3. It is estimated that the biogas flow rate has to be supplemented with natural gas over 25% of the operational time of an SOFC system (2070 h $yr^{-1}$) in order to maintain a constant average value of fuel input [24].

The techno-economic analysis performed in this study is based on an assumption of a constant average fuel input. The analysis does not include any strategy for mitigating biogas production rate fluctuations. Calculations were performed to assess the impact of natural gas blending on SOFC performance. Substituting 20% of biogas fuel energy input with natural gas at constant fuel utilization has a minor effect on the power output from an SOFC system with AGR. The concentration of methane in the fuel stream increases by 5.4% points. However, after mixing with anode exhaust gas, methane concentration in the anode feed stream does not significantly increase due to dilution with steam and carbon dioxide. The net power output from an SOFC system and the net electrical efficiency increase by 0.8% and 0.4% respectively. With the average price of natural gas for industrial users in 2011 of 5.21 \$ $GJ^{-1}$ (EIA), the additional cost of providing 20% of energy input as natural gas over 25% of operational time is estimated to have a negligible effect on the COE from an SOFC system (<0.2¢kW $h^{-1}$).

Thus, while the assumption of a constant fuel input is not representative of hourly-based operations, it provides a reasonable approximation to the annual-based techno-economic analysis presented herein. Further, introducing a short-term biogas storage system or blending with natural gas is expected to have only a minor effect on techno-economics of an SOFC system due to the low price of natural gas and high capital cost of SOFC systems.

## 5. System description

The proposed system concept implemented in Aspen Plus consists of a biogas clean-up unit, fuel and air compressors, a pre-reformer, an air preheater, a fuel cell stack, an afterburner and a heat recovery unit, as depicted in Fig. 4.

Biogas enters the system at nearly atmospheric pressure (1) and the temperature of the mesophilic digestion process (311 K). The supplied biogas is comprised of 56.6% $CH_4$, 36.7% $CO_2$, 5.8% $H_2O$ and trace amount of $N_2$. The biogas is contaminated with $H_2S$ (2.21 g $m^{-3}$) and siloxanes whose concentration is difficult to measure accurately [22]. A typical siloxane concentration in WWTF digester gas ranges from 4.64 to 36.7 mg $m^{-3}$ [21] and has to be reduced for fuel cell application. Therefore, the biogas is pretreated in a clean-up system and directed to a fuel compressor

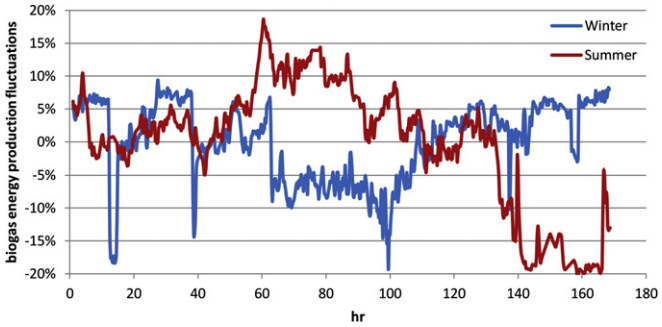


**Fig. 2.** Biogas energy production fluctuations (%) based on 1-week data sets using 15 min average values.

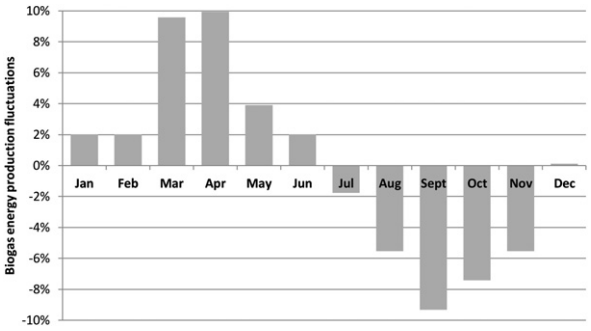


**Fig. 3.** Biogas energy production fluctuations (%) based on monthly average values.

(2). Pre-conditioned fuel is mixed in an ejector with a high temperature, rich in steam, recycled anode exhaust gas (AGR) (4). The preheated mixture is then supplied to a catalytic pre-reformer (5), where 20% of methane in the fuel is converted to hydrogen and carbon dioxide at a temperature of 923 K and a steam-to-carbon ratio (*S*/*C*) of 1.2. The heat required to maintain a constant temperature in the pre-reformer is supplied from the combustor exhaust gases (14). The pre-reformed fuel mixture is supplied to the fuel cell anode. The cathode is supplied with air preheated to 923 K using the exhaust gases downstream of the pre-reformer (15). The stack operates at an average temperature of 998 K and a fuel utilization factor (UF) of 80%. The hydrogen present in the anode exhaust (8) is catalytically oxidized in an afterburner with the oxygen depleted air exiting the cathode side (12). The energy available in the exhaust gases is used for the fuel pre-reformer, air preheater and the waste heat recovery unit (WHR). The recovered heat supplies digesters (maintaining the optimal mesophilic temperature of 311 K in the vessels) and the thermal load of onsite buildings. The DC power generated in the fuel cell stack (20) is converted to AC power in an inverter. The conditioned electric power (21) is partially used to run the fuel and air compressors (22, 23). The remaining portion of the generated power meets a portion of the electrical demand of the WWTF.

## 6. Modeling approach

The SOFC system performance is evaluated at steady state for the integration with small, medium, and large scale WWTFs. The biogas energy input for the model is constant, equal to 640 kW, 2.98 MW and 11.92 MW based on a lower heating value of methane (LHV). These input values correspond to the amount of fuel required for a 300 kW, a 1.4 MW and a 5.6 MW MCFC system operating at 47% efficiency [23]. The respective wastewater flow determined from a correlation developed based on the data from [6] is 183 $m^3\ s^{-1}$, 616 $m^3\ s^{-1}$ and 2350 $m^3\ s^{-1}$. Assuming a constant biogas energy input is a significant simplification. Biogas flow rate can vary by as much as 10% of the average flow rate value [24]. A reduced fuel pressure could cause unexpected plant shutdowns. Depending on site specific fuel flow rate fluctuations, a storage system or some supplemental natural gas fuel might be required for reliable CHP system operation. These options are not considered in this study. The balance-of-plant components are evaluated with predefined models available in Aspen Plus components library. The efficiencies of BOP equipment and pressure drops in the system components, summarized in Table 5 and Table 6 respectively, are constant and equal for all considered system sizes. The heat loss from the SOFC system equals 3% of the fuel input (LHV) with the following distribution: stack 1.5%, combustor 1%, pre-reformer 0.5%.

### 6.1. Pre-reformer

The pre-reformer is commonly employed in SOFC systems fueled with hydrocarbon fuels to partially convert the methane and higher hydrocarbons into hydrogen and carbon dioxide before the fuel cell stack. This is done in order to avoid coking and excessive local thermal gradients inside the stack, which might develop when endothermic methane reforming and exothermic hydrogen oxidation reactions occur in close vicinity. Biogas contains a significant amount of methane, therefore a pre-reformer is considered. Although it is possible to perform internal steam reforming of biogas [25,26] or gradual internal reforming of methane [27] in SOFCs, a conservative approach with 20% of external pre-reforming is assumed. The external reformer might be required for the system when methane concentration is increased due to blending biogas with natural gas or biogas quality variation. The effect of the presence of a pre-reformer on system technical performance and economics is captured in a sensitivity analysis. Pre-reforming is accomplished by catalytic steam reforming and water-gas shift reactions over a nickel catalyst according to reactions 1 and 2.

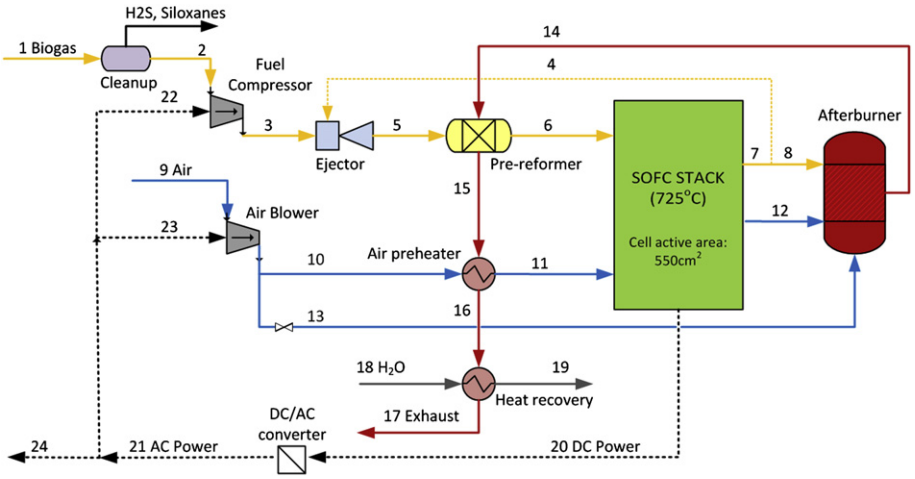


**Fig. 4.** The scheme of the proposed SOFC-based CHP system.

**Table 5**
BOP components efficiencies.

| Parameter | Value |
|---|---|
| Fuel compressor efficiency (%) | 71.3 |
| Air compressor efficiency (%) | 66.5 |
| DC/AC converter efficiency (%) | 96.0 |
| Ejector efficiency (%) | 20.0 |

$$CH_4 + H_2O \rightarrow 3H_2 + CO \quad (1)$$

$$CO + H_2O \rightarrow H_2 + CO_2 \quad (2)$$

The amount of steam supplied to the reforming process is critical for avoiding carbon deposition (which leads to deactivation of nickel catalyst) and achieving high hydrogen yield. The minimum amount of steam required for the biogas reforming under proposed operating conditions is determined with Aspen Plus. It is described with a steam-to-carbon ratio ($S/C$) which is a ratio of the molar flow of steam ($n_{H2O}$) to the total molar flow of carbon in the fuel ($n_{CH4,fuel} + n_{CO2,fuel}$), Eq. (3).

$$S/C = \frac{n_{H2O}}{n_{CH4,fuel} + n_{CO2,fuel}} \quad (3)$$

According to chemical equilibrium computations, at the operating temperature of 923 K and the given biogas composition the minimum $S/C$ equals 0.78. This number is lower than the $S/C$ ratio applied in natural gas reforming processes because of the differences in reacting mixture composition. The presence of $CO_2$ in the biogas fuel and an introduction of additional species ($H_2$, CO, $CO_2$) with anode recycled gas shift the equilibrium composition of the reacting mixture. As a result, less steam is required to ensure a carbon deposition-free operating conditions. However, carbon deposition is observed in experimental investigation of biogas reforming at theoretically sufficient steam concentration to avoid it [25]. It is suspected that the cause of this phenomenon is the presence of $H_2S$ or biogas composition fluctuations [25]. Therefore, a common practice is to supply excess steam to the reforming process. The $S/C$ for the proposed system performance simulation is 1.2.

Steam reforming is not the only possible reforming pathway for biogas. Biogas offers an opportunity of employing dry internal fuel reforming [25,28] due to the presence of $CO_2$ (Eq. (4)).

$$CH_4 + CO_2 \rightarrow 2H_2 + 2CO \quad (4)$$

However, the dry reforming reaction rate is relatively slow compared with steam reforming. As a result, cell voltage can be reduced due to significant activation overpotential [29]. Moreover, additional $CO_2$ dilution is required for a typical biogas composition (60% $CH_4$, 40% $CO_2$) to avoid carbon formation [28]. Therefore, dry reforming of biogas is not a recommended reforming method for the state-of-the-art SOFCs [25].

**Table 6**
Pressure drops in the SOFC system components.

| Component | $\Delta p$ (kPa) |
|---|---|
| Fuel cleanup unit | 10 |
| Pre-reformer (fuel/exhaust) | 2/2 |
| Stack (anode/cathode) | 2/7 |
| Air preheater (air/hot exhaust) | 10/5 |
| Afterburner | 2 |
| Heat recovery | 1 |
| Piping and valves | 5 |

### 6.2. Fuel cell stack modeling

The fuel cell stack performance is evaluated by extrapolating a single cell performance. The operating point is determined from a cell polarization curve implemented in Aspen Plus as a Fortran 77 subroutine. A single cell polarization curve accounts for activation losses ($V_{act}$) on the anode and cathode side, ohmic loss ($V_{ohm}$) and concentration loss ($V_{conc}$). The general relation between cell voltage (CV) and current density is as follows:

$$CV = E - V_{act} - V_{ohm} - V_{conc} \quad (5)$$

The open circuit voltage ($E$) is determined from the Nernst potential, Eq. (6), where the temperature dependent relation, Eq. (7) is acquired from [30].

$$E = E_o - \frac{RT}{nF}\ln\left(\frac{x_{H2O}}{x_{H2}\cdot\sqrt{x_{O2}}}\right) \quad (6)$$

$$E_o = 1.2723 - 2.7645\cdot10^{-4}\cdot T \quad (7)$$

Activation losses ($V_{acta}$, $V_{actc}$) express the voltage drop due to the reaction energy barrier. They are calculated by employing the Butler–Volmer relation, with a simplifying assumption for the activation barrier coefficient of $\alpha = 0.5$ [31]. The exchange current density, $J_o$, for anode and cathode electrodes is computed from Eqs. (8) and (9). The parameters are obtained from [30].

$$J_{oa} = \gamma\cdot x_{H2}\cdot x_{H2O}\cdot\exp\left(\frac{-E_{aa}}{RT}\right) \quad (8)$$

$$J_{oc} = \gamma\cdot x_{O2}^{0.25}\cdot\exp\left(\frac{-E_{ac}}{RT}\right) \quad (9)$$

where $x_i$ is a molar fraction of species i, $\gamma$ is an activation barrier overpotential coefficient, $E_{aa}$, $E_{ac}$ are the activation energies for the anode and cathode, $R$ is the universal gas constant and $T$ is temperature,

$$V_{act,a} = \frac{RT}{nF}\ln\left(\frac{\alpha\cdot J}{J_{oa}} + \sqrt{\left(\frac{\alpha\cdot J}{J_{oa}}\right)^2 + 1}\right) \quad (10)$$

$$V_{act,c} = \frac{RT}{nF}\ln\left(\frac{\alpha\cdot J}{J_{oc}} + \sqrt{\left(\frac{\alpha\cdot J}{J_{oc}}\right)^2 + 1}\right) \quad (11)$$

$$V_{act} = V_{act,c} + V_{act,a} \quad (12)$$

where $F$ is the Faraday constant, $J$ is current density, $J_{oa}$, $J_{oc}$ are the anodic and cathodic exchange current densities and $n$ is the number of moles of electrons generated in a reaction.

The ohmic loss due to charge transport is computed as follows:

$$V_{ohm} = J\cdot(ASR_{ohme} + ASR_{ohma} + ASR_{ohmc}) \quad (13)$$

where $ASR_{ohme}$, $ASR_{ohmc}$, $ASR_{ohma}$ are area specific resistances of the electrolyte, cathode and anode respectively.

The cell resistance is computed by summing each of the anode, electrolyte and cathode contributions as given by:

$$ASR_{ohmi} = A_i\cdot\exp\left(\frac{B_i}{T}\right)\cdot th_i \quad (14)$$

where $ASR_{ohmi}$ is the resistance, $A_i$, $B_i$ are experimental coefficients, and $th_i$ is the thickness. Thermo-physical properties and geometry are acquired from the literature [30].

Concentration losses resulting from mass transport limitations are considered through a logarithmic relation given by:

$$V_{conc} = \frac{RT}{nF}\ln\left(\frac{J_L}{J_L - J}\right) \quad (15)$$

where the limiting current density, $J_L$, is 1.6 A cm$^{-2}$ [30].

Using the SOFC cell model as given above, a model-predicted polarization curve was produced and is illustrated in Fig. 5. The performance characteristic is generated for an average stack temperature of 998 K, a fuel utilization of 0.8, and reactant concentrations that are averaged from cell inlet to outlet. The area specific resistance (ASR) under these operating conditions is approximately 0.45 Ω cm$^2$.

The operating cell voltage (CV) for system performance evaluation is 0.78 V with a respective current density ($J$) of 0.35 A cm$^{-2}$. The total active area ($A_{tot}$) is determined from Eq. (16).

$$A_{tot} = \frac{I_{tot}}{J} \quad (16)$$

Where $I_{tot}$ is the stack current evaluated from Eq. (17).

$$I_{tot} = U_{F,sys} \cdot n \cdot n_{CH4,fuel} \cdot F \quad (17)$$

where $U_{F,sys}$ is the fuel utilization factor of the system, $n$ is the number of moles of electrons, $n_{CH4,fuel}$ is the molar flow of methane, and $F$ is the Faraday constant. The total power ($P_{DC}$) from the fuel cell module is computed from Eq. (18).

$$P_{DC} = I_{tot} \cdot CV \quad (18)$$

The single cell active area is equal to 550 cm$^2$, which is the size of state-of-art planform for anode-supported, planar SOFCs [32]. Given the single cell area ($A_{cell}$), the total number of cells ($N_{cells,tot}$) required for the system (or equivalently, the total cell area required, $A_{tot}$) can be computed from specification of (1) either the net system power output or the fuel input and (2) the fuel utilization. The maximum number of cells envisioned for large SOFC stacks varies among manufacturers but the expected range is likely to span from 300 to 500 cells depending on the cell planform and gas manifolding strategy. Assuming the number of cells in a stack ($N_{cells,st}$) is equal to 400, the number of stacks ($N_{stacks}$) is computed from Eq. (19).

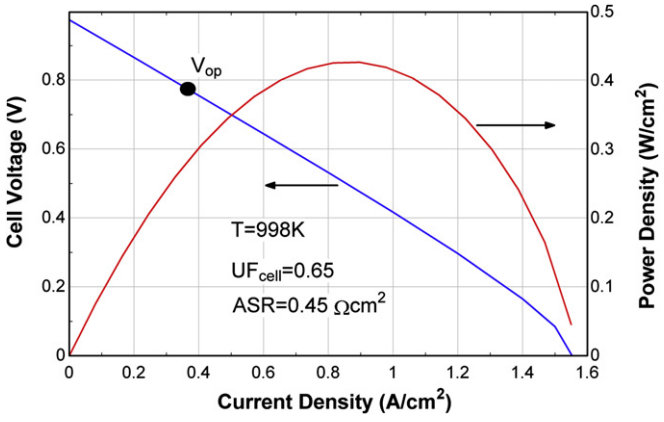


**Fig. 5.** Single cell polarization curve and power density as a function of current density for average fuel and oxygen concentrations at 998 K.

$$N_{stacks} = \frac{N_{cells,tot}}{N_{cells,st}} \quad (19)$$

With the aforementioned assumptions, the SOFC power block is comprised of sets of 60 kW stacks. The number of stacks for a small, a medium and a large scale system is 6, 30 and 119 respectively. The total number of cells required is computed based on the known total active area ($A_{tot}$) and the single cell area ($A_{cell}$) from Eq. (20)

$$N_{cells,tot} = \frac{A_{tot}}{A_{cell}} \quad (20)$$

The assumption about the number of cells in a single stack influences the number of stacks. It is intuitive to anticipate that the number of stacks will influence the system economics. However, modular system scale-up is proven not to have a significant effect on the capital cost. The capital cost is determined by the manufacturing cost, which scales with production volume (MW yr$^{-1}$) [33].

## 7. Technical performance indicators

The measures used to describe system performance are the net electrical efficiency ($\eta_{el,net}$) and the net combined heat and power efficiency ($\eta_{CHP,net}$) defined with Eqs. (21) and (22) respectively.

$$\eta_{el,net} = \frac{P_{AC,net}}{n_{CH4,fuel} \cdot LHV} \quad (21)$$

$$\eta_{CHP,net} = \frac{P_{AC,net} + Q_r}{n_{CH4,fuel} \cdot LHV} \quad (22)$$

where: $P_{AC,net}$ is the net power output (kW), $Q_r$ is the heat recovered (kW), $n_{CH4,fuel}$ is the molar flow of methane (kmol s$^{-1}$), and LHV is the lower heating value of methane (kJ kmol$^{-1}$)

## 8. Baseline system performance

The baseline system performance is evaluated at the operating point of 0.78 V and 0.35 A cm$^{-2}$ at the average stack temperature of 998 K for all considered system sizes. The fuel utilization is 80% and the extent of external methane reforming is 20% at the $S/C$ of 1.2. A summary of the SOFC system performance results for the small, the medium and the large scale biogas source is given in Table 7.

The net electrical efficiency and the CHP efficiency are equal for all system sizes. This is because the operating parameters (cell voltage, current density, temperature, $S/C$), biogas fuel composition, BOP component efficiencies and relative heat loss are equal. This behavior is in good accordance with the data for MCFCs, where the electrical efficiencies of a 300 kW, a 1.4 MW and a 2.8 MW system are equal [23]. The fuel compressor and the air blower consume 10% of the stack DC power.

## 9. Parametric study

The possibilities for system net electrical efficiency improvement are investigated by performing a parametric study. The

**Table 7**
SOFC system performance results for a small, a medium and a large scale biogas source scale.

| Scale | Small | Medium | Large |
|---|---|---|---|
| Biogas (LHV) (kW) | 640 | 2980 | 11,920 |
| Net AC Power (kW) | 330 | 1530 | 6140 |
| $Q_r$ (kW) | 230 | 1060 | 4280 |
| $\eta_{el,net}$ (%) | 51.6 | 51.6 | 51.6 |
| $\eta_{CHP,net}$ (%) | 87.5 | 87.5 | 87.5 |
| Active area (m$^2$) | 140 | 650 | 2600 |

operating parameters under analysis are the following: *S*/*C* ratio, fuel utilization on a system level, cell voltage and the extent of external reforming. The baseline values of the considered parameters together with the variation range are summarized in Table 8. In this study, the biogas fuel input is fixed and system fuel utilization is specified. Therefore, changing SOFC design parameters, such as design cell voltage, affect the size of the SOFC system (e.g., in terms of the number of cell-stacks required and the BOP). This methodology is different from design studies based on a fixed SOFC system size and varying fuel input.

### 9.1. Design cell voltage

Increasing the operating voltage at constant fuel utilization requires an increased active area and a lower operating current density. The net electrical efficiency gain resulting from increasing the cell voltage to 0.85 V is significant at 6.5% points. This is due to both increased DC power generation and decreased cooling air demand resulting from lower power density. The heat recovery decreases due to reduced heat capacity of the exhaust stream. However, the net CHP efficiency increases by 2% points. This is because the net electrical efficiency gain more than offsets the reduced heat recovery.

### 9.2. Fuel utilization

Increasing the fuel utilization (at a fixed fuel input), results in an increased power generation in the stack. The operating current density is kept constant while the cell voltage is allowed to vary. The increased total current is accommodated by increasing the total active area by increasing the number of SOFC cells and stacks. As a result of increased power generation (at a fixed fuel input), the net electrical efficiency increases. There are a few additional phenomena affecting the net electrical efficiency resulting from a change in fuel utilization. Firstly, increased fuel utilization is accompanied by increased parasitic power. This is because of increased cooling air requirement due to increased heat generation in oxidation reactions. Moreover, the average reactant concentrations decrease, which results in a decreased cell voltage. Increased fuel utilization, however, results in a higher steam concentration in the anode exhaust, thus reducing the recycling rate and fuel compression required for the ejector. There is an overall increase of 2.1% points in net electrical efficiency due to an increase in fuel utilization to 87.5%. The heat recovery decreases with increased fuel utilization as there is less fuel available in the combustor. Moreover, there is more heat required for the reformer as a result of reduced AGR. The net CHP efficiency decreases by 2.4% points with an increase in fuel utilization to 87.5%.

### 9.3. Steam-to-carbon ratio

As shown in Fig. 6, the system net electrical efficiency increases by 1.8% points with decreasing the *S*/*C* ratio to 0.8. Steam is supplied by anode gas recycling, thus the *S*/*C* ratio is decreased by reducing the amount of recycled gas. With less recycling, the fuel mixture is less diluted with the products of anodic reactions and cell voltage increases. Moreover, the volumetric flow of recycled stream entrained in an ejector decreases from 54% to 44% of the anode exhaust gas. This is followed by a reduced fuel compression required for the ejector. Despite increased electrical efficiency, the CHP efficiency decreases by 0.1%. This is due to a decreased heat recovery with more heat being supplied from the hot exhaust to the reformer to maintain a constant temperature of 923 K. This increased heat requirement stems from a lower fuel mixture temperature at the reformer inlet due to decreased AGR.

**Table 8**
A summary of the parametric study input.

| Parameter | Baseline | Range |
|---|---|---|
| Steam-to-carbon ratio | 1.2 | 0.8–1.6 |
| Fuel utilization (%) | 80.0 | 72.5–87.5 |
| % External reforming (%) | 20.0 | 0.0–30.0 |
| Cell voltage (*V*) | 0.78 | 0.7–0.85 |

### 9.4. External reforming

Decreasing the extent of external reforming brings the benefit of combining the endothermic reforming reaction with exothermic fuel oxidation within the stack. Therefore, the cooling air requirement decreases. Reduced parasitic power results in an increased net electrical efficiency. Eliminating the external reforming results in a net efficiency increase by 1.2% points. The heat recovery increases with a decreased external reforming. This is because less heat is required for the pre-reformer. The net CHP efficiency increases by 2% points as the external reforming is eliminated.

## 10. Economic analysis methodology

The economics of the proposed SOFC system is evaluated with the cost of electricity ($COE_{CHP}$) and the cost of heat ($COH_{CHP}$). The COE is chosen for being a convenient indicator for comparing the economics of the SOFC system with competing cogeneration technologies. This comparison is made as a part of the economic viability assessment process. The COE and COH are determined by evaluating Eqs. (23) and (24).

$$COE_{CHP} = \frac{R_f C_{sys,el}}{CF_e A_p} + \frac{C_{maint,el}}{CF_e A_p} + \frac{F_{biogas}}{\eta_{el,net}} - \frac{(\eta_{CHP,net} - \eta_{el,net}) F_{ng}}{\eta_{el,net}\eta_{ng}} \quad (23)$$

$$COH_{CHP} = \frac{R_f C_{sys,whr}}{CF_e A_p} + \frac{C_{maint,whr}}{CF_e A_p} + \frac{(\eta_{CHP,net} - \eta_{el,net}) F_{ng}}{\eta_{el,net}\eta_{ng}} \quad (24)$$

where $R_f$ is the capital recovery factor, $CF_e$ is the capacity factor, $A_p$ is the plant availability, $F_{biogas}$, $F_{ng}$ is the biogas and natural gas fuel cost (\$ kW $h^{-1}$), $\eta_{el,net}$, $\eta_{CHP,net}$ are the net electrical efficiency and CHP efficiency respectively, $C_{sys,el}$, $C_{sys,whr}$ is the unit installed cost of the SOFC system and the waste heat recovery unit respectively, and $C_{maint,el}$ , $C_{maint,whr}$ is the maintenance cost of the power generation unit and the waste heat recovery unit respectively. The capacity factor and plant availability factor the SOFC system are 90% [19] and 99.5% [34]. They are equal for all system sizes. The influence of the capacity factor on system economics is captured in a sensitivity analysis. The biogas cost is assumed to be zero for the baseline system economic performance evaluation. This is a common assumption justified by biogas being a byproduct of wastewater treatment process [24]. However, in some studies biogas is assigned a cost [35]. Therefore, the effect of introducing a biogas cost on the proposed system economics is considered in a sensitivity analysis. The natural gas fuel cost is equal to the average natural gas price for industrial users (large-scale facilities) and commercial users (small-scale facilities) in 2011 of 0.017 \$ kW $h^{-1}$ and 0.03 \$ kW $h^{-1}$ respectively (EIA). The maintenance cost of the SOFC-stack is evaluated assuming a stack replacement every 5 years [34]. The maintenance cost for other system components is 5% of the installed cost of these components, which is comparable

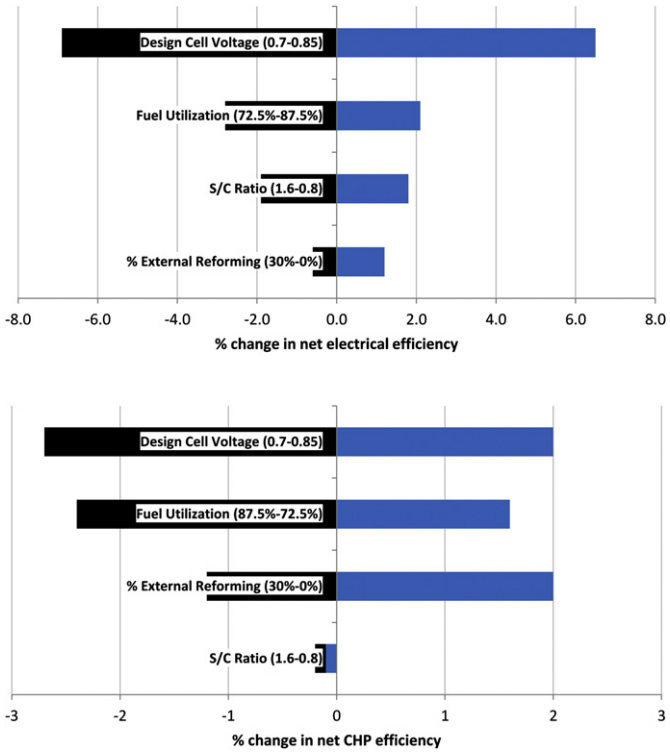


**Fig. 6.** Tornado charts showing the sensitivity of the net electrical efficiency (left) and the net CHP efficiency (right) to the change in design cell voltage, $S/C$, $U_{F,sys}$ and the % external reforming.

with assumptions made in other economic studies [36,37]. This maintenance cost includes the replacement of catalysts for the reformer, the afterburner and the biogas clean-up system. The computed maintenance cost for the small, the medium and the large scale SOFC system is 0.016 \$ kW $h^{-1}$, 0.012 \$ kW $h^{-1}$ and 0.009 \$ kW $h^{-1}$ respectively. The total project cost of the proposed SOFC system is evaluated with a bottom-up costing method with an uncertainty of ±30% [38]. The capital recovery factor for the total project cost is evaluated assuming a 10% discount rate and the project lifetime of 20 years. The bottom-up costing method is illustrated in Fig. 7.

The total project cost (TPC) consists of the total installed cost (TIC) and indirect costs (IDC). The TIC is comprised of the cost of purchased equipment, shipping cost, and the installation and commissioning cost. The indirect costs include the cost of engineering (13% TIC), construction (14% TIC), and legal and construction fees (9% TIC) [39]. The system installed cost is determined by adding the cost of purchased equipment and the installation cost of individual system components. The costs of the individual components are reported in 2011 U.S. dollars if not stated otherwise. The Chemical Engineering Plant Cost Index (CEPCI) is used for conversion between cost data years, if necessary. The installed cost of the SOFC system was determined from the cost of individual components acquired from the literature or evaluated with Aspen Plus Economic evaluation tool, Table 9.

The cost of compressors, blowers, burners and the heat recovery units for all system sizes is evaluated with Aspen Plus Economic Evaluation Tool. The size and materials required for the components are determined by the software based on the flow sheet simulation results. The biogas pretreatment system cost is evaluated by scaling a unit cost of a system employed for biogas conditioning for MCFC applications [19]. The reformer cost is evaluated based on a unit cost and scaling law presented in Ref. [40]. The cost of a fuel cell stack is determined based on a unit cost of 1620 US \$ $m^{-2}$ at a production volume of 100 MW $yr^{-1}$ [33]. This number reflects the manufacturing cost of mature anode-supported, planar cells with metallic interconnects. The unit cost also accounts for a 10% reduction of the stack cost due to scale-up of the cell active area from 125 $cm^2$ to 550 $cm^2$, as suggested by Thijssen [33]. The cost reduction is assigned to a reduced number of cells required for the stack and a reduction in the inactive area

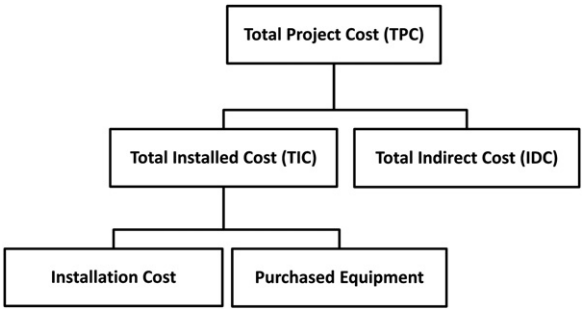


**Fig. 7.** The bottom-up system costing diagram.

**Table 9**
Unit cost of the SOFC system components.

| Component | Scaling law | Baseline cost ($C_o$) | Installation factor | Source |
|---|---|---|---|---|
| Stack | $C_o A_{active,tot}$ | 1620 \$ $m^{-2}$ | 1.42 | [33,40] |
| Inverter | $C_o P_{DC}$ | 169 \$ $kW^{-1}$ | 1.42 | [37] |
| Biogas Pretreat | $C_o V_{biogas}$ | 71,154 (\$ $m^{-3}$ N $h^{-1}$) | – | [19] |
| Reformer | $C_o(m_{H2}/1125)^{0.7}$ | 204 (k \$ kg $H_2^{-1}$-day) | 1.1 | [40] |
| Compressors | – | – | – | AspenPlus |
| Heat exchangers | – | – | – | AspenPlus |
| Burner | – | – | – | AspenPlus |

**Table 10**
A summary of a small, a medium and a large scale SOFC system component costs (in thousands of 2011 US$).

| | Scale | | |
|---|---|---|---|
| Component | Small | Medium | Large |
| Stack and inverter | 387 | 1794 | 7183 |
| Reformer | 37 | 108 | 264 |
| Burner | 14 | 67 | 268 |
| Compressors, blowers | 422 | 1118 | 2397 |
| Heat exchangers | 155 | 659 | 1622 |
| Pretreatment | 355 | 1908 | 3825 |
| Indirect cost | 505 | 2091 | 5825 |
| Total project cost | 1907 | 5991 | 22,004 |
| Unit installed cost ($2011 kW$^{-1}$) | 5780 | 3916 | 3584 |

relative to the total cell area. Expressing the unit cost of a stack in ($ m$^{-2}$) instead of commonly used ($ kW$^{-1}$) is dictated by biogas characteristics. Due to fuel dilution from digester gas $CO_2$ content, a stack operates at a lower power density compared with a natural gas-fueled system. Therefore, a larger active area is necessary to ensure a required power output is achieved. The cost of an SOFC stack can vary with the production volume between 150 and 1500 US $ kW$^{-1}$ [37]. At a power density of 0.273 W cm$^{-2}$, the respective unit cost is between 409 and 4090 US $ m$^{-2}$. The uncertainty related to the assumption of the unit stack cost ($ m$^{-2}$) is accounted for in a sensitivity analysis.

## 11. Economic results

The summary of the total installed cost (TIC) of individual system components and indirect cost for all system sizes is presented in Table 10. The SOFC system costing results indicate that the unit installed cost ($ kW$^{-1}$) decreases with the system size from 5780 $ kW$^{-1}$ for a small system (330 kW) to 3584 $ kW$^{-1}$ for a large system (6 MW). Based on the capital cost and maintenance cost estimates, the baseline COE for the small, the medium, and the large scale is 0.079 $ kW h$^{-1}$, 0.058 $ kW h$^{-1}$ and 0.050 $ kW h$^{-1}$, respectively. The average annual grid electricity price for industrial users in 2011 reported by EIA is 0.07 $ kW h$^{-1}$. The small scale system should be compared against the grid electricity price for commercial users of 0.103 $ kW h$^{-1}$ (EIA 2011). The COE from a medium and a large scale SOFC system is competitive with the grid electricity price for industrial users. The small system is competitive with the average grid electricity for commercial users, but would require incentives to successfully compete against the grid, if considered as an industrial user. The computed baseline COH for the small, the medium, and the large scale is 0.031 $ kW h$^{-1}$, 0.017 $ kW h$^{-1}$ and 0.016 $ kW h$^{-1}$, respectively. If natural gas is used onsite to generate heat at a WWTF in an 83% efficient boiler, the cost of heat is 0.036 $ kW h$^{-1}$, 0.021 $ kW h$^{-1}$ and 0.021 $ kW h$^{-1}$ (exclusive of boiler capital cost and maintenance). Therefore, using the low cost waste heat instead reduces the plant operational costs. The COH is lower for larger systems due to a lower unit natural gas price ($ kW h$^{-1}$).

**Table 11**
Summary of the parameters considered in the sensitivity analysis.

| Parameter | Baseline | Range |
|---|---|---|
| Unit project cost ($ kW$^{-1}$) | 5780/3916/3584 | ±30% |
| Biogas cost ($ kW h$^{-1}$LHV) | 0 | 0–0.01 |
| Steam-to-carbon ratio | 1.2 | 0.8–1.6 |
| Fuel utilization (%) | 80 | 72.5%–87.5% |
| External reforming (%) | 20 | 0–30 |
| Capacity factor (%) | 90 | ±5% |
| Design cell voltage ($V$) | 0.78 | 0.7–0.85 |

## 12. Sensitivity analysis

The baseline COE is subjected to a sensitivity analysis in order to evaluate the influence on system economics of the following parameters: capital investment, capacity factor, biogas cost, and operating parameters ($S/C$, $U_{F,sys}$, %ER, CV). The baseline parameter values and variation range considered for the parametric study are summarized in Table 11. The price of biogas is determined from the annual average natural gas price for industrial users in 2011 from the EIA database. Only the methane content in biogas is assigned a value. The results of sensitivity analysis for small, medium, and large scale WWTFs are shown in Fig. 8a–c respectively.

### 12.1. The impact of economic parameters on COE

The COE is highly sensitive to the unit project cost. Decreasing the system capital cost could potentially reduce the COE by around 32%. The strong impact of the capital cost on COE is a result of the zero biogas fuel cost. Introducing a biogas cost of 0.01 $ kW h$^{-1}$ (LHV) could increase the COE by as much as 40% for a large scale system. The small scale system is less sensitive to the biogas cost compared with the medium- and large-scale systems because it is the most capital intensive. If biogas cost is introduced, SOFC systems are still competitive with the grid.

### 12.2. The impact of operating parameters on COE

Increasing the capacity factor (defined as the ratio of the actual electricity generation to the maximum electricity production from a system) by 5% could reduce the COE by 8%, as electricity generation increases at constant capital investment cost, maintenance cost and system efficiency. The system economics could be also improved by decreasing the steam-to-carbon ratio (defined in Section 5), eliminating external reforming, decreasing the fuel utilization factor and decreasing cell voltage. Increasing cell voltage to 0.85 V causes a COE increase of 30%, 34% and 39% for a small-, medium- and a large SOFC system respectively. The increase of the COE is caused by an increased SOFC stack and inverter cost with an increased active area and power output. This effect has much higher impact on the system cost than the decreased cost of the air blower and the air preheater. An additional increase of the COE is due to reduction of the heat generation credit (last term in Eq. (23)). This reduction stems from a net electrical efficiency gain of 6.5%. Operating at a lower steam-to-carbon ratio improves the economics because the cost of the pre-reformer and the cost of the fuel compressor decrease. Reducing the external reforming is beneficial for reducing the cost of the pre-reformer, the air blower and the air preheater. Therefore, eliminating the external reforming results in the COE reduction by 6%. Decreasing the fuel utilization factor (defined as the fraction of fuel input converted to power within the SOFC stack) to 72.5%, results in a COE reduction by 10%. This is because the cost of the following components is reduced: the fuel cell stack, the air blower, the air preheater, and the pre-reformer. The COE reduction is enhanced by an increase in heat generation credit (last term in Eq. (23)) due to reduced net electrical efficiency.

## 13. Comparison of COE from different cogeneration technologies

In order to be implemented at WWTFs, the SOFC-based cogeneration system has to offer both the technical and economic benefits compared with other cogeneration technologies. The analysis results indicate that the net electrical efficiency of an SOFC system fueled with biogas could be as high as 51.6% (LHV). This number is significantly higher compared with the electrical efficiencies of

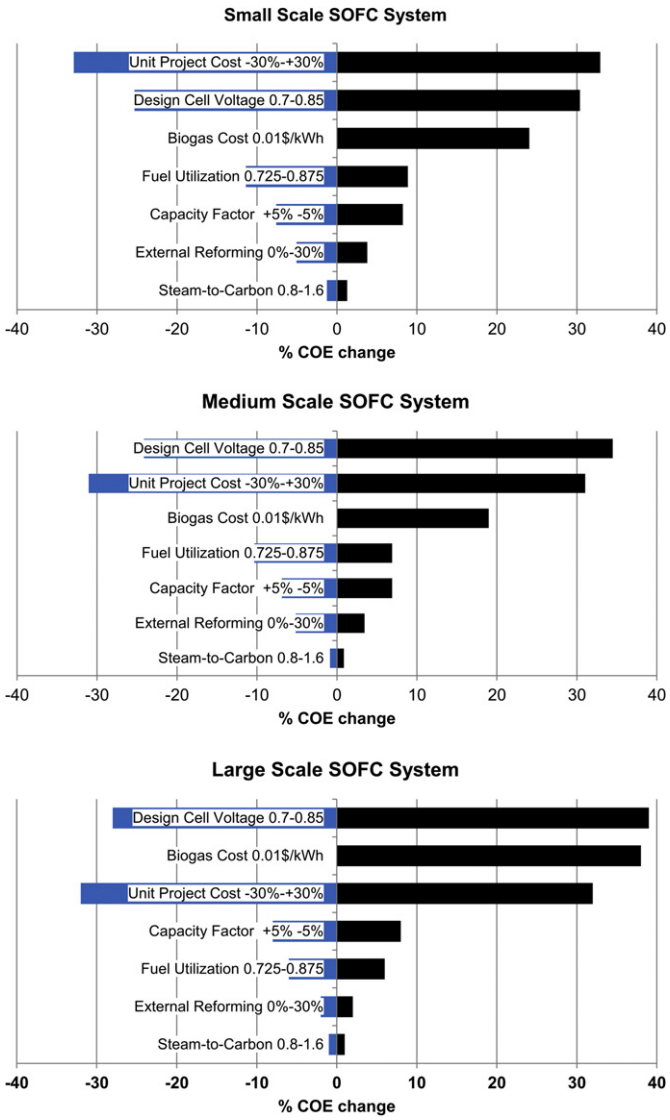


**Fig. 8.** Tornado charts showing the sensitivity of the COE from a small scale, a medium scale and a large scale biogas-fueled SOFC system to chosen parameters.

reciprocating engines, gas turbines or MCFCs presented in Table 2. Biogas initially seems to be an economically attractive fuel due to its low cost. However, the intrinsic contaminants often impose an installation of an extensive biogas pretreatment system, which has an adverse effect on the economics. The comparison of COE range is made based on literature data and manufacturer specifications for a small biogas source (640 $kW_{LHV}$), a medium biogas source (2.97 $MW_{LHV}$) and a large biogas source (11.92 $MW_{LHV}$). The biogas energy input is equal to the input used for the SOFC system performance evaluation. Based on the given energy input, a reciprocating engine, a gas turbine and a MCFC system is chosen. The efficiency and subsequently the power output for each technology is estimated based on the manufacturer specifications. A correction accounting for the low calorific value of biogas is made where necessary. The capital cost for each technology is estimated based on unit costs from literature sources summarized in Table 12. Since biogas fuel is site specific, the high-end and the low-end values were used to determine the range of the cost electricity from each system at small-, medium- and large scale.

The capital cost of a required biogas pretreatment system is assumed to vary between \$500–\$3,000 $kW^{-1}$ as proposed in Ref. [41] for all the technologies. The indirect cost of each system is estimated as a fraction of installed cost as proposed in Ref. [39]. The following assumptions about economic factors are made for all the systems: lifetime of 20 years, discount rate of 10%, capital recovery factor of 12%, capacity factor range of 90–95%, biogas cost range of 0.00–0.01 \$ $kW\ h^{-1}_{LHV}$. The plant availability factor is 90–96% for reciprocating engines [2], 95–97% for gas turbines [2] and 90–95% for MCFCs and SOFCs [2]. The maintenance cost varies between \$0.01–\$0.045 $kW\ h^{-1}$ for reciprocating engines [41], 0.008–0.01 \$ $kW\ h^{-1}$ for gas turbines [2], and 0.004–0.019 \$ $kW\ h^{-1}$ for MCFCs and SOFCs [2]. The cost of electricity for each technology is evaluated from Eq. (23). The range of the COE for different technologies is summarized in Table 13.

The estimated COE generally decreases with an increased system size. This is because of the economy of scale which means that the unit cost of a system decreases with an increased system size. Comparing the estimated COE from medium- and large-scale facilities with the average U.S. grid electricity price for industrial users in 2011 of 0.07 \$ $kW\ h^{-1}$ (EIA), leads to a conclusion that large systems ($\sim$3–6 $MW_{el}$) could successfully compete against the grid without any incentives. Gas turbines are the most economically

**Table 12**
Summary of performance indicators and unit cost of reciprocating engines, microturbines, gas turbines and MCFCs.

| Technology | Recip. Engines | Microturbines | Gas turbines | MCFCs |
|---|---|---|---|---|
| *Small scale* | | | | |
| Fuel input $_{LHV}$ (kW) | 640 | 640 | NA | 640 |
| Power (kW) | 154 | 160 | NA | 300 |
| $\eta_{electrical}$ (% $_{LHV}$) | 24 [42] | 25 [43] | NA | 44–47 [18,23] |
| $\eta_{CHP}$(% $_{LHV}$) | 71–87 [2] | 66 [41] | NA | 70–85 [2] |
| Equipment ($ kW$^{-1}$) | 1428 [43] | 1350 [43] | NA | 5500 [44] |
| *Medium scale* | | | | |
| Fuel input $_{LHV}$ (kW) | 2980 | 2980 | 2980 | 2980 |
| Power (kW) | 1067 | 851 | 516 | 1400 |
| $\eta_{electrical}$ (% $_{LHV}$) | 35.8 [45] | 28.6 [43] | 17.3 [46] | 44–47 [18,23] |
| $\eta_{CHP}$(% $_{LHV}$) | 71–87 [2] | 62.1 [43] | 66–86 [2] | 70–85 [2] |
| Equipment ($ kW$^{-1}$) | 1222 [43] | 1100 [43] | 1330 [43] | 4200 [44] |
| *Large scale* | | | | |
| Fuel input $_{LHV}$ (kW) | 11,920 | 11,920 | 11,920 | 11,920 |
| Power (kW) | 5006 | 3406 | 3242 | 5600 |
| $\eta_{electrical}$ (% $_{LHV}$) | 42 [47] | 28.6 [43] | 27.2 [48] | 44–47 [18,23] |
| $\eta_{CHP}$ (% $_{LHV}$) | 71–87 [2] | 62.1 [43] | 66–86 [2] | 70–85 [2] |
| Equipment ($ kW$^{-1}$) | 933 [43] | 1100 [43] | 665 [48] | 3500 [44] |
| *All sizes* | | | | |
| Cleanup ($ kW$^{-1}$) | 500–3000 [41] | 500–3000 [41] | 500–3000 [41] | 500–3000 [41] |
| O&M ($/kW h) | 0.01–0.045 [41] | 0.012–0.025 [2] | 0.008–0.01 [2] | 0.004–0.019 [2] |
| Availability (%) | 90–96 [2] | 85–90 [2] | 95–97 [2] | 90–95 [2] |
| CF (%) | 90–95 | 90–95 | 90–95 | 90–95 |
| Biogas cost ($ kW h$^{-1}$) | 0–0.01 | 0–0.01 | 0–0.01 | 0–0.01 |

attractive technology for large scale applications. At the small scale, all the considered technologies could be competitive with the 2011 average grid electricity price for commercial users in the U.S. of 0.103 $ kW h$^{-1}$ (EIA). SOFCs are competitive with other cogeneration technologies due to their high electrical efficiency. The modeling results show that mature SOFCs could successfully compete against other technologies and the grid electricity price. However, the viability of integrating a CHP system with a biogas source is site specific and depends on biogas composition, contaminants concentration, and local utility pricing.

## 14. Conclusions

In this paper, a techno-economic analysis of SOFC-based CHP systems for biogas utilization at WWTFs is performed. Based on system modeling results and cost estimates the following conclusions are drawn:

**Table 13**
Comparison of the COE for different cogeneration technologies for WWTFs.

| COE ($ kW h$^{-1}$) | Small | Medium | Large |
|---|---|---|---|
| Reciprocating engines | 0.091–0.173 | 0.062–0.199 | 0.045–0.185 |
| Microturbines | 0.070–202 | 0.071–0.204 | 0.071–0.204 |
| Gas turbines | NA | 0.034–0.132 | 0.028–0.118 |
| MCFC | 0.064–0.166 | 0.058–0.153 | 0.047–0.142 |
| SOFC | 0.057–0.145 | 0.047–0.143 | 0.042–0.134 |

- The proposed SOFC-based cogeneration system concept for WWTFs offers a net electrical efficiency of 51.6% (LHV). This efficiency is equal for the case of an integration with a small (640 kW$_{LHV}$), medium (2.98 MW$_{LHV}$) and a large (11.92 MW$_{LHV}$) biogas source. SOFC systems fueled with biogas could achieve significantly higher net electrical efficiency compared with competing cogeneration technologies, such as: reciprocating engines, gas turbines, microturbines and MCFCs.
- The net electrical efficiency of the proposed SOFC system concept could be further increased by 6.5% points by increasing cell voltage to 0.85 V, 2.1% points by increasing fuel utilization to 0.875, 1.8% points by decreasing steam-to-carbon ratio to 0.8 and 1.2% points by eliminating the external pre-reformer.
- The SOFC system cost estimates indicate that the unit installed cost ($ kW$^{-1}$) decreases with the system size from 5780 $ kW$^{-1}$ for a small system (330 kWe) to 3584 $ kW$^{-1}$ for a large system (6 MWe).
- Based on the capital cost and maintenance cost estimates, the baseline COE for the small, the medium, and the large scale is 0.079 $ kW h$^{-1}$, 0.058 $ kW h$^{-1}$ and 0.05 $ kW h$^{-1}$, respectively. A comparison with the average annual grid electricity price for industrial users and commercial users in the U.S. in 2011 of 0.07 $ kW h$^{-1}$ and 0.103 $ kW h$^{-1}$ respectively (EIA) shows that SOFC systems are competitive with the grid electricity price.
- The sensitivity analysis of the COE from SOFC systems indicates that introducing the biogas cost would result in an increase of the COE from a small, medium and a large SOFC system by 24%, 19% and 38% respectively. The impact of biogas cost on COE for medium and large facilities increases with system size since it becomes less capital intensive. The small scale systems do not follow this pattern due to different utility pricing.
- Decreasing the capital cost of an SOFC system by 30% results in a COE reduction by 32% at all system sizes. The strong impact of the capital cost on the COE is a result of zero fuel cost.
- Further COE reduction can be achieved by optimizing the operating parameters of the proposed SOFC system concept, such as: 6% COE reduction by eliminating external fuel reforming due to lower system cost and parasitic power, 8% COE reduction by increasing the capacity factor by 5% or 10% COE reduction by decreasing the fuel utilization.
- The COE increases by 30%, 34% and 39% for a small-, medium- and a large-scale SOFC system respectively with an increase in cell voltage to 0.85 V. Increasing the cell voltage requires a significant increase in active area. This causes an increase in the stack cost. The COE cost increase is further enhanced by reducing the value of a heat generation credit stemming from a net electrical efficiency gain of 6.5% points.
- A comparison between different cogeneration technologies for WWTFs shows that larger systems present a lower COE and are more economically favorable due to a lower unit capital cost. Gas turbines are the most economically attractive for large-scale applications, given the SOFC configuration studied here.
- The COE from a CHP system operated at a WWTF can vary over a wide range. The viability of integrating any CHP system with a biogas source is site specific and strongly depends on biogas quality, contaminants concentration, local utility pricing and local incentives.

SOFCs offer an efficient way of utilizing biogas fuel at WWTFs and could successfully compete with other cogeneration technologies in this market if mature stack costs are realized. The local characteristics of biogas fuel, however, make the economics of CHP projects in WWTFs site specific, and highly variable. While not explored in this study, other SOFC system enhancements, such as

gas turbine integration deserve exploration and may significantly increase the efficiency performance and offer further economic incentive to adopt the technology, particularly for system sizes above 1 MWe.

## Acknowledgments

The authors would like to thank Mr. John Kuosman and Ms. Wendy Anderson from the Denver Metro Wastewater Reclamation District for plant operational information. Funding for this work was provided by the U.S. Department of Energy, Office of Energy Efficiency & Renewable Energy (EERE) under contract number DE-FG36-08GO88100.

## Nomenclature

| | |
|---|---|
| $S/C$ | steam to carbon ratio |
| $n_{H2O}$ | molar flow of water (moles-s$^{-1}$) |
| $n_{CO2,fuel}$ | molar flow of carbon dioxide (moles-s$^{-1}$) |
| $n_{CH4,fuel}$ | molar flow of methane (moles-s$^{-1}$) |
| CV | cell voltage(V) |
| E | nernst voltage (V) |
| $V_{act}$ | activation voltage loss (V) |
| $V_{ohm}$ | ohmic voltage loss (V) |
| $V_{conc}$ | concentration voltage loss (V) |
| $E_o$ | reference voltage (V) |
| $R$ | universal gas constant (J mol$^{-1}$ K$^{-1}$) |
| $T$ | cell temperature (°C) |
| $F$ | Faraday's constant (J mol$^{-1}$) |
| $n$ | number of electrons per mol |
| $x_i$ | molar fraction of component i (kPa) |
| $E_{aa}$ | anode activation energy (J) |
| $J_{oa}$ | anode exchange current density (A cm$^{-2}$) |
| $\gamma$ | activation overpotential factor (A cm$^{-2}$) |
| $E_{ac}$ | cathode activation energy (J) |
| $J_{oc}$ | cathode exchange current density (A cm$^{-2}$) |
| $J$ | current density (A cm$^{-2}$) |
| $ASR_{ohm}$ | area specific resistance (Ω cm$^2$) |
| $th_i$ | thickness of component I (μm) |
| $j_L$ | limiting current density (A cm$^{-2}$) |
| $A_{tot}$ | total SOFC active area required (cm$^2$) |
| $I_{tot}$ | total current (A) |
| $U_{F,sys}$ | system fuel utilization coefficient |
| $P_{DC}$ | gross DC power from SOFC (kW) |
| $N_{cells,tot}$ | total number of cells |
| $A_{cell}$ | area of a cell (cm$^2$) |
| $N_{stacks}$ | number of stacks |
| $N_{cells,st}$ | number of cells in a stack |
| LHV | lower heating value (kW) |
| $\eta_{el,net}$ | net electrical efficiency |
| $\eta_{CHP,net}$ | net combined heat and power efficiency |
| $P_{AC,net}$ | net AC power output (kW) |
| $Q_r$ | heat recovery (kW) |
| $COE_{CHP}$ | cost of electricity ($ kW h$^{-1}$) |
| $COH_{CHP}$ | cost of heat ($ kW h$^{-1}$) |
| $R_f$ | capital recovery factor |
| $C_{sys,el}$ | unit capital cost of the system ($ kW$^{-1}$) |
| $C_{maint,el}$ | maintenance cost ($ kW h$^{-1}$) |
| $F_{biogas}$ | biogas cost ($ kW h$^{-1}$) |
| $F_{ng}$ | natural gas cost ($ kW h$^{-1}$) |
| $\eta_{ng}$ | natural gas fueled boiler efficiency |
| $CF_e$ | capacity factor |
| $A_p$ | availability factor |
| $C_{sys,whr}$ | unit capital cost of the heat recovery ($ kW$^{-1}$) |
| $C_{maint,whr}$ | maintenance cost of the heat recovery ($ kW h$^{-1}$) |
| WWTF | wastewater treatment facility |
| RFS | renewable fuel standards |
| RIN | renewable identification number |
| CHP | combined heat and power |

## References

[1] J. Daly, T. Leo, C. Pais, R. Venkataraman, J. Wang, M. Farooque, ECS Transactions 30 (2011) 261–270.
[2] Brown, Caldwell, Evaluation of Combined Heat and Power Technologies for Wastewater Facilities, Columbus Water Works, Columbus, 2010, EPA 832-R-10–006.
[3] M. Noponen, T. Hottinen, C.E. Sandstrom, WFC20 Biogas Unit Operation, Biogas Workshop, Lund, presentation, 2011.
[4] P. Holtberg, J. Conti, Emissions of Greenhouse Gases in the United States 2009, U.S. Energy Information Administration, Washington DC, 2011.
[5] U.S. Environmental Protection Agency Combined Heat and Power Partnership, Opportunities for Combined Heat and Power at Wastewater Treatment Facilities:Market Analysis and Lessons from the Field (2011).
[6] M.B. Sullivan, Economic and Non-Economic Benefits of Implementing Cogeneration at a Municipal WPCF, Carollo Engineers (personal communication).
[7] T. J. D'Andrea, The Changing Economics of Landfill Gas/Biogas: Back to Basics?, Presentation at the International Biomass Conference and Expo, Denver, 2012.
[8] J.L. Preston, R.J. Spiegel, Journal of Power Sources 86 (2000) 283–288.
[9] J. Laurencin, M. Petitjean, J. Fouletier, F. Lefebvre-Joud, K. Girona, ECS Transactions 25 (2009) 1041–1050.
[10] A.E. Richards, A. Colclasure, W. Rosensteel, N.P. Sullivan, D.M. Murphy, ECS Transactions 35 (2011) 2653–2667.
[11] J.Z. Staniforth, R.M. Ormerod, C.J. Laycock, ECS Transactions 16 (2009) 177–188.
[12] J.W. Zondlo, M. Gong, F. Elizalde-Blancas, X. Liu, I.B. Celik, C. Xu, Journal of Power Sources 195 (2010) 4583–4592.
[13] T. Oshima, K. Sasaki, Y. Shiratori, International Journal of Hydrogen Energy 33 (2008) 6316–6321.
[14] M. Jahn, A. Michaelis, R. Näke, A. Weder, M. Heddrich, Simple and robust biogas-fed SOFC system with 50% electric efficiency-Modeling and Experimental results, in: 10th European SOFC forum, Lucerne (2012).
[15] Y. Yoo, F. Hamdullahpur, S. Farhad, Journal of Power Sources 195 (2010) 1446–1453.
[16] F. Maréchal, S. Leuenberger, D. Favrat, J. Van herle, Journal of Power Sources 118 (2003) 375–383.
[17] *Fuel Cell Today*, "6 MW Bloom Fuel Cell Installation to Provide Prime Power for eBays New Data Center," www.fuelcelltoday.com, 21 June 2012. Available at: http://www.fuelcelltoday.com/news-events/news-archive/2012/june/6-mw-bloom-fuel-cell-installation-to-provide-prime-power-for-ebay%E2%80%99s-new-data-centre (accessed February 2013).
[18] Bob Bucher, Final Report King County Fuel Cell Demonstration Project, King County Wastewater Treatment Division, Seattle, 2009.
[19] J.H.P. Yoon, S.W. Nam, I. Oh, D.K. Choi, S.A. Song, Journal of Electrochemical Science and Technology (2010) 102–111.
[20] Don Beverly, White paper, Treatment Solutions for Landfill Gas Fuel Applications, Xebec, 2007, Available at: http://wwwxebecinc.com/pdf/e_white_paper.pdf (accessed February 2013).
[21] J.H. Jun, J.H. Jun, B.S. Ahn, K.H. Park, D.S. Choi, J.Y. Park, T.H. Kim, J.G. Lee, ECS Transactions 5 (2007) 733–738.
[22] M. Nourot, personal communication regarding experience with a Desiccant Siloxane Removal System, Fortistar Methane Group, 2008.
[23] FuelCell Energy, DFC300, DFC1500, and DFC3000 product brochures. Available at: http://www.fuelcellenergy.com/products.php (accessed February 2013).
[24] J. Kuosman, W. Anderson, Cogen Performance Report, Metro Wastewater Reclamation District Denver Colorado, Internal Memorandum 2010.
[25] P. Leone, A. Lanzini, International Journal of Hydrogen Energy 35 (2010) 2463–2476.
[26] Y. Lin, Z. Zhan, J. Liu, S.A. Barnett, Solid State Ionics 176 (2005) 1827–1835.
[27] J.M. Klein, M. Hénault, C. Roux, Y. Bultel, S. Georges, Journal of Power Sources 193 (2009) 331–337.
[28] T. Ijichi, T. Oshima, K. Sasaki, Y. Shiratori, International Journal of Hydrogen Energy 35 (2010) 7905–7912.
[29] V. Kiousis, L. Nalbandian, I.V. Yentekakis, G. Goula, Solid State Ionics 177 (2006) 2119–2123.
[30] A. Corradetti, R. Bove, P. Lunghi, P. Lisbona, Electrochimica Acta 53 (2007) 1920–1930.
[31] S.W. Cha, W. Cholella, B.F. Prinz, R.P. O'Hayre, Fuel Cell Fundamentals, John Wiley & Sons, Inc, New York, USA, 2009.
[32] E. Tang, M. Pastula, B. Borglum, ECS Transactions 35 (2011) 63–69.
[33] J. H. J. S. Thijssen, The Impact of Scale-up and Production Volume on SOFC Manufacturing Cost, Technical report, Pittzburgh, 2007.
[34] R.J. Braun, Journal of Fuel Cell Science and Technology 7 (2010).
[35] J.L. Silveira, I. Aparecida de Castro Villela, Applied Thermal Engineering 25 (2005) 1141–1152.
[36] M. Korpas, A.T. Holen, C.J. Greiner, International Journal of Hydrogen Energy 32 (2007) 1500–1507.

[37] C. Mabilat, M. Zahid, A. Brisse, L. Gautier, Q. Fu, Energy & Environmental Science 3 (2010) 1382–1397.
[38] K.D. Timmerhaus, R.E. West, M.S. Peters, Plant Design and Economics for Chemical Engineers, fifth ed., McGraw-Hill Companies Inc, New York, 2003.
[39] A. Aden, T. Eggeman, M. Ringer, B. Wallace, J. Jechura, P. Spath, Biomass to Hydrogen Production Detailed Design and Economics Utilizing the Battelle Columbus Laboratory Indirectly Heated Gasifier. Denver, Technical Report NREL/TP-510–37408 (2005).
[40] W.L. Becker, R.J. Braun, M. Penev, M. Melaina, Journal of Power Sources 200 (2012) 34–44.
[41] P Lemar, CHP and Bioenergy Systems for Landfills and Wastewater Treatment Plants. 2007, Available at: http://www1.eere.energy.gov/manufacturing/distributedenergy/pdfs/chp_and_bioenergy_pt2.pdf (accessed February 2013).
[42] Caterpillar, Inc., CAT G3412 Gas Engine product brochure. Available at: http://www.cat.com/cda/files/2692328/7/LEHE0293-00.pdf (accessed February 2013).
[43] EPA Combined Heat and Power Partnership, Biomass CHP Catalogue of Technologies, EPA, 2007.
[44] R. Remick, Molten Carbonate and Phosphoric Acid Stationary Fuel Cells. Overview and Gap Analysis (2010). NREL, Golden, TP-56049072.
[45] Caterpillar Inc., CAT Gas Generator Set Ratings, product brochure. Available at: http://www.cat.com/cda/files/3683800/7/Cat%20Gas%20Genset%20Ratings%20Efficiencies%20LEXE0422-03.pdf (accessed February 2013).
[46] Kawasaki, Gas Turbines Americas, GPB06 product brochure. Available at: http://www.kawasakigasturbines.com/files/Kawasaki_GPB06.pdf (accessed February 2013).
[47] GE-Energy, Jenbacher Type 6 Gas Engine product brochure. GE Jenbacher type 6, Available at: http://www.hoyrytys.fi/brochure/GE%20Jenbacher%20620%20series.pdf (accessed February 2013).
[48] Robert Farmer, Gas Turbine World, Handbook, Pequot Publishing, 2006.